

**Sensitization of p-GaP (100) Photoelectrodes With CdSe
Quantum Dots**

by

Shichen Lian

Department of Chemistry

University of Michigan

Undergraduate Thesis Advisor: Professor Stephen Maldonado

This thesis has been read and approved by

_____.

Date: ____/____/2014

Acknowledgements

My undergraduate career at the University of Michigan has been an enjoyable and adventurous one. A hands-on research oriented journey in the field of chemistry for the past two years has both broadened my understanding of nature and shaped my career goal. I want to thank my undergraduate research advisor Professor Stephen Maldonado for allowing me to learn from and work for him. As an educator, he brought me to the world of semiconductor photoelectrochemistry, which I immediately became hooked. As a mentor, he stimulated my enthusiasm in fundamental scientific research and I have decided to continue my journey of life in chemistry graduate school. None of the work would have been produced without his support. I also want to thank Professor John Wolfe for his help during the writing process of this thesis.

I also want to thank our former postdoc Dr. Zhijie Wang for teaching me photoelectrochemical measurements and fundamental theories of semiconductor nanocrystals. The knowledge I have gained from him has played a significant role when I performed research independently in my senior year. Additionally, I am also grateful for all the members in Professor Maldonado's research group especially Ms. Betsy Brown, Mr. Eli Fahrenkrug, and Mr. Junsi Gu, who have helped me both in instruments and understanding of fundamental theories.

Studying abroad in undergraduate level can be both rewarding and frustrating. I want to thank all my friends for keeping me company and making my homesickness fade away. Their friendship not only has supported me emotionally, but also helped me sharpen my English skills and blend in with the American culture. The academic atmosphere at Professor Maldonado's laboratory and the well-balanced social

environment at the University of Michigan have helped me become both an independent scientific researcher and an independent individual.

None of the stories of my past four years would have happened without my parents' support. Their financial and mental supports have made my adventure in US possible. Regardless of the physical distance between China and US, they have always been there with me. I plan to continue to make them proud.

Abstract

This thesis contains two sections of my undergraduate research. Chapter one is dedicated to demonstrate a light-stimulated hole injection process by using p-GaP(100) photoelectrodes and CdSe quantum dots. The valence band edge of CdSe is higher than the valence band edge of p-GaP. After excitation of light, the photoinduced hole in the valence band of CdSe is thermodynamically possible to be injected into the valence band of GaP. A series of systematic electrochemical measurements including photoresponse, time-resolved photoluminescence decays, and steady-state current-potential responses have indicated the occurrence of such quantum dots sensitized hole injection processes.

The excitonic peak of the wet-chemically synthesized CdSe quantum dots locates around 560 nm; however, the photoresponse position of p-GaP photoelectrode is also locating around that wavelength. Namely, this similarity makes it challenging to deconvolute the spectral signatures of the GaP substrate and the CdSe sensitizer. Chapter two demonstrates my work focusing on surface modification of CdSe quantum dots in order to shift the excitonic dynamics. When the size of quantum dots is too small, hole injection processes cannot be demonstrated with photoresponse measurement because the spectral profile of GaP and CdSe will be convoluted in external quantum yield spectra. With ligand exchanging procedures inspired from literatures, the CdSe sensitization peaks have shown a bathochromic shift, well out of the spectral signatures of the GaP substrate. UV-Vis spectroscopy, fluorescence spectroscopy, and NMR spectroscopy have been used to show the redshifted exciton peak and characterize the synthesized surface ligands. Photoresponse measurement is used to demonstrate the same hole injection process in chapter one.

List of Figures

Figure 1.1. a) Time-resolved photoluminescence decays measured from adsorbed CdSe quantum dots (diameter = 4.5 nm) on (red line) glass and (green line) p-GaP(100), respectively. Pulsed excitation wavelength = 561 nm. b) Steady-state current-potential responses for a (black lines) mirror-polished, bare p-GaP(100) photoelectrode and (green lines) a mirror-polished p-GaP(100) photoelectrode with adsorbed CdSe quantum dots (diameter = 4.5 nm). Responses both (dashed lines) in absence of any illumination and (solid lines) under monochromatic illumination at 605 nm at 0.33 mW cm^{-2} are shown. c) External quantum yield spectra for (black) a bare p-GaP(100) photoelectrode and (green) a p-GaP(100) photoelectrode coated with a monolayer of CdSe quantum dots. Inset: Absorption spectrum for the same CdSe quantum dots dispersed in hexane. d) Schematic depiction of sensitized hole injection from a CdSe quantum dot into p-GaP.....Page 10

Figure 1.2. a) External quantum yield spectra for a textured p-GaP(100) photoelectrode sensitized with CdSe quantum dots (diameter = 4.5 nm) after various quantum dot surface treatments. b) External quantum yield for a textured p-GaP(100) photoelectrodes sensitized with CdSe quantum dot cores (diameter = 3.7 nm) coated with ZnSe. The shell thicknesses were controlled through variation in the ZnSe shell growth time.....Page 11

Figure 2.1. Schematic demonstration of coupling effect between the HOMO of PTC (PTC-electron withdrawing group and PTC-electron donating group) and the valence band edge of CdSe QDs.....Page 16

Figure 2.2. a) UV-Vis absorption spectra of CdSe quantum dots with TOPO native ligand (black line) and with PTC ligands in different concentrations. b) External quantum yield spectra for (black) a p-GaP (100) photoelectrode coated with a layer of CdSe with ethyldiamine ligand (black) and phenyldithiocarbamate ligand (red). c) External quantum yield difference between p-GaP/CdSe-EDA and p-GaP/CdSe-PTC.....Page 20

Figure 2.3. a) Time-resolved photoluminescence decays measured from adsorbed CdSe quantum dots with TOPO native ligands on (red line) GaP and on (black line) glass. b,c,e,f) Fluorescence image of CdSe on glass, GaP, CdSe-PTC on glass, and GaP. d) Time-resolved photoluminescence decays measured from adsorbed CdSe quantum dots with PTC ligands on (red line) glass and on (black line) GaP.....Page 21

Figure 2.4. a) UV-Vis absorption spectra of CdSe quantum dots with TOPO native ligand (black line) and with PTC ligands in different concentrations. b) External quantum yield spectra for (black) a bare p-GaP (100) photoelectrode (black line) and a p-GaP (100) photoelectrode coated with a layer of CdSe with ethyldiamine ligand (red) and PTC ligand (blue).....Page 23

Figure 2.5. a) UV-Vis absorption spectra of CdSe quantum dots with TOPO native ligand (black line) and with F-PTC ligands in different concentrations. b) External quantum yield spectra for (black) a p-GaP (100) CdSe-TOPO photoelectrode and a p-GaP (100) photoelectrode coated with a layer of CdSe with FPTC (red).....Page 24

Table of Content

Acknowledgement.....	ii
Abstract.....	iv
List of Figures.....	v, vi
Table of Content.....	vii
Chapter 1. Sensitization of p-GaP (100) photoelectrode with CdSe Quantum Dots: Light stimulated hole injection.....	2
1.1 Introduction	
1.2 Materials and methods	
1.3 Results and Discussions	
1.4 Conclusions	
Chapter 2. Tuning Sensitization photoresponse of p-GaP/CdSe pair by phenyldithiocarbamate surface ligand.....	11
2.1 Introduction	
2.2 Materials and methods	
2.3 Results and Discussions	
2.4 Conclusions	
Reference.....	25
Appendix.....	28
C ¹³ NMR Characterization of PTC molecules and derivatives	
Absorption, photoluminescence spectra for CdSe/ZnSe Core/Shell Quantum dots	
XRD pattern for CdSe/ZnSe Core/Shell Quantum dot	

CHAPTER 1

Sensitization of p-GaP (100) photoelectrode with CdSe Quantum Dots: Light stimulated hole injection¹

1.1 Introduction

Photosensitization of semiconductor photoelectrodes has been a main method to utilize solar energy among current photoelectrochemical studies¹⁻⁵. In such hetero-structure systems, a light-absorbing material, which generates an electron-hole pair, is deposited onto a semiconductor photoelectrode. The photo-induced electron and hole quickly separate into two different phases, and these charge carriers are transported via a redox couple and collected by respective electrodes³. One example of such photovoltaic devices is dye-sensitized solar cell, where dye molecules are the light absorbers deposited onto semiconductor photoelectrodes (mainly TiO₂)^{2, 6-12}. Nevertheless, the relatively low energy conversion efficiency and absorption coefficients among dye-sensitized solar cells have stimulated the need to seek new photo-absorber materials¹³⁻¹⁴.

Semiconductor nanocrystals (Quantum Dots) have attracted much attention due to their large extinction coefficients, tunable band gap, and well-established synthetic strategies^{3, 5, 15-16}. Due to the quantum confinement effect, intrinsic optical band gaps of these semiconductor materials can be tuned by changing the size of synthesized particles in order to maximum solar photon absorption¹⁷⁻¹⁸. Due to these benefits of QDs, instead of dye sensitization, QDs sensitization of semiconductor photoelectrodes has been explored by many research groups¹⁹⁻²².

¹ Portions of this chapter were published in Wang, Z.; Shakya, A.; Gu, J.; Lian, S.; Maldonado, S. *J. Am. Chem. Soc.* **2013**, *135* (25), 9275-9278

Several studies have demonstrated sensitization of a semiconductor photoelectrode by using the light-stimulated electron transfer from the conduction of a quantum dot to the conduction band of metal oxides^{1, 20, 23}. Nevertheless, photoelectrochemical studies involving quantum dots sensitization on the hole injection part are still poorly explored, which can be attributed to the difficulty in finding viable combination of materials that is thermodynamically possible to inject light-excited hole from the valence band of a quantum dot to the valence band of semiconductor photoelectrode. Inspired by several literatures regarding dye sensitization based on hole injection processes of planar p-type GaP photoelectrodes, the possibility of using p-GaP and quantum dots to demonstrate hole injection have been explored in this study^{2, 7}.

The valence band edge potential of GaP has been reported to be +1.0 V vs Ag/AgCl, which is more negative than that of CdSe^{2, 7, 24-25}. This feature suggests that hole injection from a CdSe quantum dot into p-GaP should be thermodynamically possible.

In this study, wet-chemically synthesized CdSe quantum dots were surface-absorbed onto p-GaP (100) photoelectrodes. The native surface ligands of colloidal quantum dots (trioctylphosphine oxide and oleate species) were exchanged with more conductive organic ligands such as ethylenediamine in order to increase the external quantum yield signals. A combination of optical characterization, photoresponse measurement, time-resolved photoluminescence decay measurement, and steady-state current-potential responses techniques has been utilized to demonstrate the light-stimulated hole injection process.

A control experiment was also performed in order to comprehensively study the proposed hole injection mechanism. Type I CdSe/ZnSe core/shell quantum dots were

synthesized and used to sensitize the p-GaP (100) photoelectrodes. In a Type I core/shell quantum dots, the valence and conduction band edge of the shell material is respectively higher and lower than the valence and conduction band edge of the core material. After shining light on p-GaP/CdSe/ZnSe pair, hypothetically, all the photoinduced excitons should be confined within CdSe core. In external quantum yield spectra, no additional photoresponse signals should be observed apart from the GaP's intrinsic profile.

1.2 Materials and methods

Materials and Chemicals

Selenium powder (Se, $\geq 99.5\%$), 1-octadecene (ODE, $\geq 99.5\%$), cadmium acetate dehydrate ($\text{Cd}(\text{CH}_3\text{CO}_2)_2$, $\geq 98\%$), oleic acid (OA, $\geq 99.0\%$), trioctylphosphine oxide (TOPO, 90%), zinc stearate (technical grade), trioctylphosphine (TOP, 90%), ethylenediamine (EDA, $\geq 99.5\%$), potassium chloride (KCl, $\geq 99\%$), (3-aminopropyl)triethoxysilane ($\geq 98\%$), heptanes (99%), isopropanol ($\geq 99.7\%$), toluene (99.8%), dodecylamine (99%) and ammonium sulfide ($(\text{NH}_4)_2\text{S}$, 20% in H_2O) were used as received from Sigma Aldrich. Europium (III) chloride (EuCl_3 , 99.9%) was obtained from Strem Chemicals. Methanol (99.8%) and acetone (99.5%) were obtained from VWR International. Hexanes (98.5%) and 40% v/v NH_4F (aq) were purchased from MARCRON Chemicals and Transene, respectively. Chloroform (99.9%) and concentrated HCl (aq) were obtained from Fisher Scientific. Silver print was from GC Electronics. H_2O was purified ($>18 \text{ M}\Omega \text{ cm}$) with a Barnstead Nanopure III purifier and used throughout. N_2 (g), Ar (g) and forming gas (5% H_2 in N_2) were obtained from Metro Welding. GaP photoelectrodes were prepared from a 500 μm thick, single-crystalline, single-side polished p-GaP(100) wafer doped with Zn at $5.0 \times 10^{17} \text{ cm}^{-3}$. GaP wafers were obtained and used as received from ITME. Epoxy was purchased from Hysol C.

Synthesis of CdSe quantum dots

CdSe quantum dots were prepared using a modified approach reported by Peng et al.²⁶⁻²⁷ 0.047g Se powder and 7.092 g ODE were put in a 50 ml three-necked round-bottom flask and purged under Ar flow with constant stirring for 30 min. A 25 ml

Erlenmeyer flask containing 0.1596 g $\text{Cd}(\text{CH}_3\text{CO}_2)_2$ and 3 ml OA was purged under N_2 flow with constant stirring. The Se/ODE mixture was then heated to 280 °C using a heating mantle and the temperature was monitored by a thermocouple until the Se powder was completely dissolved and a pale yellow solution was generated. The $\text{Cd}(\text{CH}_3\text{CO}_2)_2$ and OA mixture was heated on a hot plate until ~120 °C and injected into the Se/ODE mixture. Within 2-3 min of injection, the solution turned orange indicating the nucleation of quantum dots and the color became deeper with increasing reaction time. After cooling to room temperature, the quantum dots were purified with a combination of methanol and acetone three times respectively. The final quantum dots were dispersed in hexanes for characterization.

Synthesis of CdSe/ZnSe core/shell quantum dots

CdSe/ZnSe quantum dots were synthesized using procedures reported by Bard et al.²⁸ 6 g TOPO and 0.05 g $\text{Cd}(\text{CH}_3\text{CO}_2)_2$ were put in a three-necked round-bottom flask and heated to 140 °C with continuous purging with Ar flow. The temperature was kept at 140 °C for 1 hr and then increased to 330 °C. 2.4 mL of 1M Se in TOP solution was injected into the hot cadmium solution. The instant color change suggested the nucleation of CdSe quantum dots. Quantum dots were purified with the same procedure mentioned above and finally dispersed in heptanes. 3 g TOPO and 2 g dodecylamine were placed in a three-necked flask, degassed with Ar and heated to 150 °C. After 1 hr, 6 mL of CdSe in heptanes solution was added into the flask with slowly injected Zn precursor solution (0.2 g Zn stearate in 2.5 mL toluene and 0.03 g Se in 2.5 mL TOP). The core/shell quantum

dots were purified using the same procedure as described above and dispersed in chloroform for optical and photoelectrochemistry measurements.

Preparation of p-GaP electrodes

One side polished 500 μm thick single crystal p-GaP(100) wafer with doping density of $5 \times 10^{17} \text{ cm}^{-3}$ was diced into $0.5 \text{ cm} \times 0.5 \text{ cm}$ squares. Ohmic contact was prepared by etching the backside of wafer briefly (30 s) with concentrated NH_4F (aq), rinsing with water, soldering a thin, even film of pure indium on the back, and then annealing in forming gas for 10 min at $400 \text{ }^\circ\text{C}$. Electrodes were prepared by attaching the GaP section (using silver print) onto a copper wire coil threaded through a glass tube and sealing with inert epoxy. Electrode areas were defined by the edge of the epoxy and were nominally 0.2 cm^2 .

Preparation of CdSe-sensitized and CdSe/ZnSe-sensitized p-GaP electrode

The p-GaP electrode was first etched using concentrated HCl for 30 s and then merged in HCl-neutralized $(\text{NH}_4)_2\text{S}$ for 6 hrs, rinsed with water, and dried with N_2 . The electrode was merged in CdSe quantum dots hexanes solution (or CdSe/ZnSe chloroform solution) for 20 min. The loosely attached quantum dots were removed by rinsing with hexanes (CdSe/ZnSe using chloroform) and soaking in hexanes (CdSe/ZnSe using chloroform) for 20 min. Finally, the quantum dots sensitized p-GaP electrode was soaked in 10% v/v EDA methanol solution for 10 min for ligand exchange before being used for photoelectrochemical measurements.

Photoelectrochemical and spectroscopic measurements

Photoelectrochemical measurements were conducted in an airtight quartz cell with an optically flat bottom. A Pt counter electrode and an Ag/AgCl reference electrode were used. Aqueous solution containing 0.1 M KCl & 0.002 M EuCl₃ were adopted as the electrolyte. The electrolyte was purged with N₂ flow when measurements were conducted. External quantum yield was measured with an Oriel 150 W Xe arc lamp (Newport) and a quarter-turn single-grating monochromator (Newport). Sample measurements were recorded with chopped illumination (20 Hz), and a quartz beam splitter was used to simultaneously record the light output intensity with a separate Si photodiode (Newport) to adjust the fluctuations in lamp intensity. The potential of the working photoelectrode was set to -0.6 V vs Ag/AgCl, and the absolute photocurrents were measured by a digital PAR 273 potentiostat. The output current signal was connected to a Stanford Instruments SR830 lock-in amplifier, and the output signals from the lock-in amplifier and the reference Si photodiode were fed into a computer controlled by custom-written LabVIEW software. Current-potential curves were measured using the digital PAR 273 potentiostat under the unchopped illumination from the monochromator.

Absorption spectra were obtained with a Varian Cary 5000 ultraviolet–visible–near-infrared (UV–Vis–NIR) photospectrometer. Luminescence spectra were measured using Fluoromax-2 Fluorimeter. Luminescence lifetime spectroscopy was measured using ALBA microscope system from ISS (Illinois) combining fluorescence lifetime imaging (FLIM, FRET) with fluorescence fluctuation spectroscopy (FCS, FCCS, FCH) capabilities. A monolayer of CdSe quantum dots on glass was prepared following the

same procedure with that on p-GaP, the glass was pretreated by soaking in 10% v/v (3-aminopropyl)triethoxysilane isopropanol solution overnight.

1.3 Results and discussions

Figure 1.1 d illustrates a schematic depiction of sensitized hole injection process from a CdSe QD to p-GaP. Theoretically, the valence band position of CdSe is lower than the valence band position of p-GaP. After shining light on the p-GaP/CdSe pair, remaining holes in the valence band of CdSe should be injected into the valence band of GaP. Figure 1.1 a shows two representative time-resolved photoluminescence decays after pulsed excitation at 561 nm. When deposited onto insulating glass, CdSe QDs capped with ethylenediamine exhibited an average decay time of 8.8 ns; when surface absorbed onto p-GaP wafer, CdSe QDs showed an average decay time of 1.4 ns, with nearly an 4-fold decrease. The decreased PL lifetime indicates that a new fluorescence-quenching pathway has been generated. Exciton relaxation can be accelerated due to the hole injection processes happened at the interface between CdSe and GaP.

Figure 1.1 b contains representative steady-state photoelectrochemical response for CdSd/p-GaP pairs. Under illumination with sub-bandgap monochromatic light (605 nm), an enhanced photocurrent has been observed compared with the bare p-GaP photoelectrodes under illumination.

Figure 1.1 c is the wavelength-dependent external quantum yield for photoelectrodes fabricated with CdSe-EDA QDs. The inset figure is the absorption spectrum for the QDs that are absorbed onto the surface of GaP. After sensitization (green curve), an increased external quantum yield values were observed with a qualitatively matched wavelength

range with the absorption profile of CdSe. Compared with bare p-GaP photoelectrodes, the observed additional signals beyond 550 nm should be attributed to the injected photoinduced hole coming from CdSe QDs.

The combination of these data strongly suggest that CdSe QDs are able to inject light stimulated hole in to p-GaP photoelectrodes.

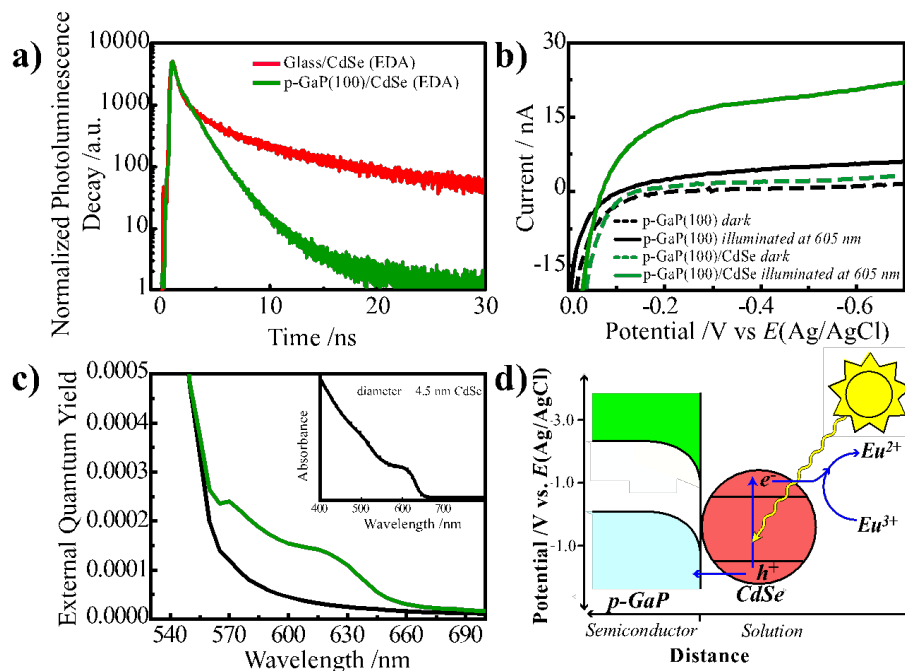


Figure 1.1². a) Time-resolved photoluminescence decays measured from adsorbed CdSe quantum dots (diameter = 4.5 nm) on (red line) glass and (green line) p-GaP(100), respectively. Pulsed excitation wavelength = 561 nm. b) Steady-state current-potential responses for a (black lines) mirror-polished, bare p-GaP(100) photoelectrode and (green lines) a mirror-polished p-GaP(100) photoelectrode with adsorbed CdSe quantum dots (diameter = 4.5 nm). Responses both (dashed lines) in absence of any illumination and (solid lines) under monochromatic illumination at 605 nm at 0.33 mW cm⁻² are shown. c) External quantum yield spectra for (black) a bare p-GaP(100) photoelectrode and (green) a p-GaP(100) photoelectrode coated with a monolayer of CdSe quantum dots. Inset: Absorption spectrum for the same CdSe quantum dots dispersed in hexane. d) Schematic depiction of sensitized hole injection from a CdSe quantum dot into p-GaP.

² Reprinted with permission from (Wang, Z.; Shakyia, A.; Gu, J.; Lian, S.; Maldonado, S. *J. Am. Chem. Soc.* **2013**, *135* (25), 9275-9278). Copyright (2014) American Chemical Society

In order to comprehensively study the hole injection mechanism, a control experiment was also performed with type I core/shell CdSe/ZnSe quantum dots. In a Type I core/shell system, the conduction and valence band edge energies for ZnSe extend both above and below the conduction and valence band-edge energies for CdSe respectively. After excitation of light, hypothetically all the photoinduced excitons will be confined within the CdSe core based on fundamental thermodynamic theories. Hence, the hole injection process should be forbidden. Figure 3 b shows that the sensitization signals from p-GaP/CdSe decreases with the increasing thicknesses of ZnSe shells, which is consistent with the proposed hypothesis. The ZnSe shell here works as an additional barrier, which blocks charge carriers from being transferred between the CdSe core and GaP. Compared with previous studies, in the p-GaP/CdSe system, the photoinduced hole should be able to transfer as the proposed mechanism (from the valence band of CdSe into the valence band of GaP).

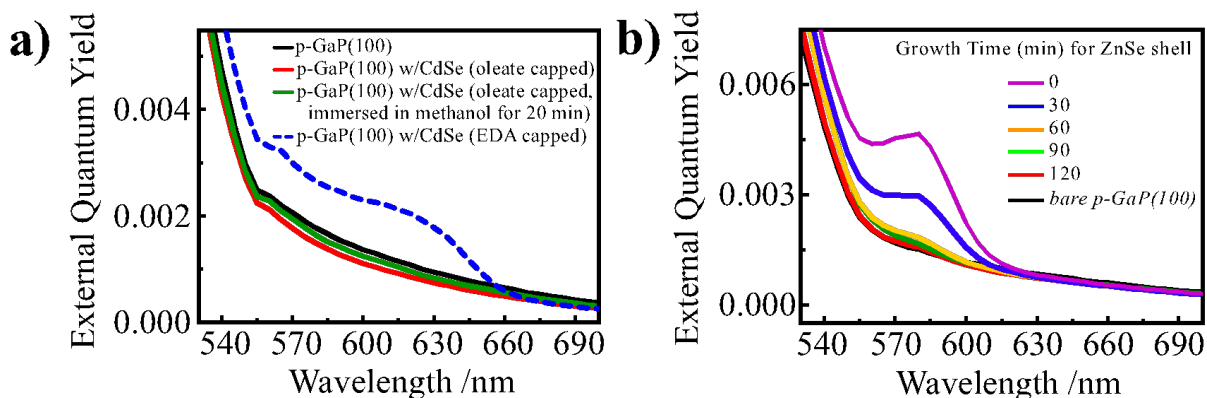


Figure 1.2³. a) External quantum yield spectra for a textured p-GaP(100) photoelectrode sensitized with CdSe quantum dots (diameter = 4.5 nm) after various quantum dot surface treatments. b) External quantum yield for a textured p-GaP(100) photoelectrodes sensitized with CdSe quantum dot cores (diameter = 3.7 nm) coated with ZnSe. The shell thicknesses were controlled through variation in the ZnSe shell growth time.

³ Reprinted with permission from (Wang, Z.; Shakya, A.; Gu, J.; Lian, S.; Maldonado, S. *J. Am. Chem. Soc.* **2013**, *135* (25), 9275-9278). Copyright (2014) American Chemical Society

1.4 Conclusion

A systematic collection of optical and electrochemical measurements have demonstrated that p-GaP and CdSe QDs is a viable combination of materials to demonstrate hole injection processes from the valence band of CdSe into the valence band of p-GaP. Before CdSe being surface absorbed onto GaP photoelectrode, apart from its own photoresponse signature, there was no observable photoresponse beyond 550 nm; after CdSe sensitization, external quantum yield measurements indicated that additional charge carriers have been collected beyond the GaP's optical band range, which should be attributed to the photoinduced hole injected from CdSe. Based on the optical studies of CdSe, the excitonic dynamic profile is also consistent between the absorption spectra and external quantum yield measurements.

CHAPTER 2

Tuning sensitization photoresponse of p-GaP/CdSe pair by phenyldithiocarbamate surface ligand

2.1 Introduction

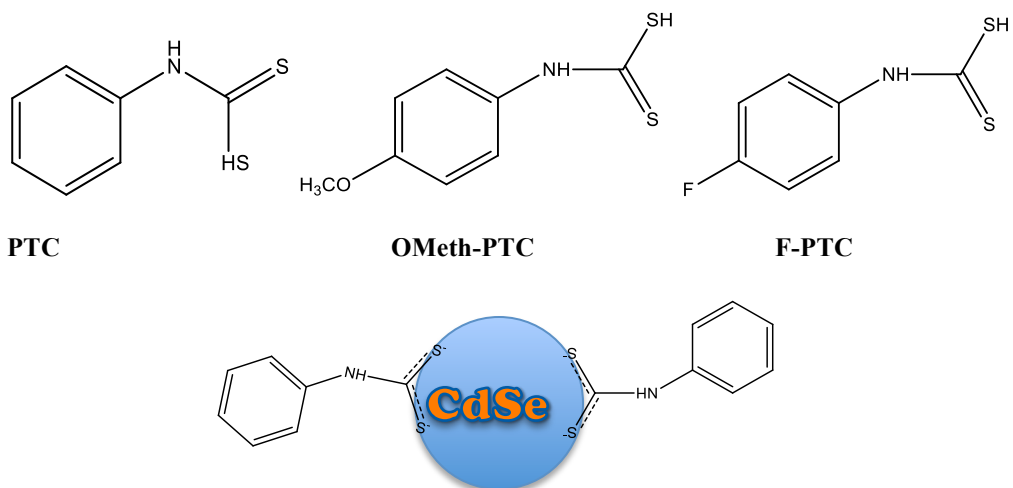
Due to the nature of synthetic systems, colloidal semiconductor nanocrystals (Quantum Dots) usually are passivated with long-chain aliphatic compounds (stearic acid and oleic acid)^{26, 29-31}. The most established method is the so-called hot-injection technique³²⁻³³. It involves the rapid injection of metal precursors into a hot solvent dissolved with another inorganic precursor. The subsequent temperature drop controls the nucleation and growth of QDs³⁴. Typical organic solvents for this system are oleic acid, n-octadecylphosphonic acid, alkylphosphines and alkylphosphine oxides³⁵. Such organic molecules will adhere to the surface of growing crystals to facilitate the kinetics of nucleation and growth, prevent the semiconductor nanocrystal core from oxidation, and control the shape of QDs. Bawendi et al. has demonstrated a systematic method to synthesize uniformly monodispersed nanocrystals by using a combination of long-chain alkylphosphines, alkylphosphine oxides, and alkylamines organic compounds³². Nevertheless, the non-conductive long carbon chains in such systems can also compromise charge transfer processes in the system of interest because they separate individual nanocrystals to prevent efficient charge transport, induce charge trapping, and complicate the surface chemistry of QDs^{30-31, 36}. Hence, numerous researchers have attempted to study how these surfactant organic molecules can impact the morphology, electronic properties, and chemical functionalities of QDs so that they can chemically functionalize these nanostructured materials^{1, 28, 30, 36-38}. Weiss has reported several roles

of organic molecules in terms of controlling the growth, surface structure, and redox activity of colloidal semiconductor nanocrystals³⁸⁻⁴³. According to her account, in the “hot-injection” reaction mixture, using long-carbon-chain organic molecules can control the shape of metal-chalcogenide QDs. Bulky alkylphosphines such as trioctylphosphine can confine the growth of QDs in three dimension in order to prevent crystal defects³⁸. Interestingly, organic surfactant molecules can impact not only the shape and composition of final products, but also the absorption and photoluminescence of QDs. When the highest occupied molecular orbital (HOMO) of the organic surface ligand couples with the HOMO of QDs, the anti-bonding orbital of this coupling, along with the lowest occupied molecular orbital (LUMO) of QDs will determine the new optical band gap of the QD’s material^{39, 41}.

Previously, we have demonstrated a light stimulated hole injection process from a CdSe quantum dot to a p-GaP photoelectrode⁵. In that study, the excitonic peak of CdSe is centered at 560 nm, which is similar to the native absorption of the planar GaP substrate. Namely, this similarity makes it challenging to deconvolute the spectral signatures of the GaP substrate and the CdSe sensitizer. Weiss et al. has demonstrated a ligand exchange procedure, which uses phenyldithiocarbamate (PTC) ligand to control hole delocalization in QDs through coupling effect between the HOMO of PTC and the valence band edge of CdSe QDs³⁹. In that study, a bathochromic shift up to 220 meV in the optical bandgap of CdSe induced by PTC has been observed. Leveraging this ligand exchange procedure, a photoelectrochemical study of the p-GaP/CdSe pair, along with the surface modification of colloidal CdSe QDs has been performed in this chapter. The native ligands (TOPO) of wet-chemically synthesized CdSe QDs have been exchanged

with PTC molecules and para-substituted derivatives of PTC. Subsequently, the surface modified CdSe QDs have been further used to sensitize p-GaP (100) photoelectrode. As what figure 2.1 depicting, theoretically, the HOMO of PTC can be coupled with the valence band edge of CdSe. The newly formed band gap of CdSe-PTC is the energy difference between hybrid anti-bonding orbital and the conduction band edge of CdSe. If the PTC molecule is para-substituted with an electron-withdrawing group, the inductive effect can lower the HOMO energy level of PTC. Hypothetically, the coupling effect should be stronger so that the bathochromic shift should be more severe. If the PTC molecule is para-substituted with an electron-donating group, the HOMO energy level of PTC should be increased. The coupling effect should lead to a less obvious bathochromic shift.

In this study, PTC, PTC-OMeth, and PTC-F (shown in table 1) have been synthesized and exchanged with the native TOPO ligand of CdSe quantum dots. UV-Vis spectroscopy was utilized to study the excitation dynamics. Furthermore, the surface modified CdSe QDs were used to sensitize p-GaP (100) photoelectrodes. Quantum yield and photoluminescence decay measurements were used to demonstrate hole injection processes from the valence band of CdSe QDs to the valence band of GaP.



Schematic 1. Synthesized PTC molecular structures and PTC molecule-CdSe quantum dots linkage demonstration.

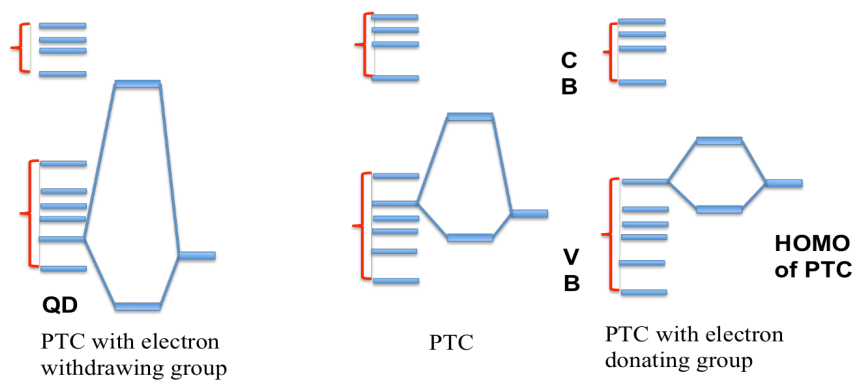


Figure 2.1. Schematic demonstration of coupling effect between the HOMO of PTC (PTC-electron withdrawing group and PTC-electron donating group) and the valence band edge of CdSe QDs.

2.2 Materials and methods

Synthesis of CdSe quantum dots

CdSe quantum dots were prepared using a modified method reported by Weiss et al⁴⁰. A 50 ml three-necked round-bottom flask containing 7.76 g of trioctylphosphine oxide, 7.76 g of hexadecylamine, and cadmium acetate (0.660 mmol) was purged under Ar flow with constant stirring for 60 min in 150 °C. One arm of the flask was left open to remove any remaining water in the system. After that, the flask was sealed and heated up to 330 °C. After the Cadmium precursor was completely dissolved in the reaction mixture, trioctylphosphine selenide solution (4mL of 1 M solution) was rapidly injected and the reaction mixture was immediately cooled to room temperature. The resulting products were purified by methanol and re-dispersed in hexanes.

Synthesis of dithiocarbamate ligands

NH₄X-PTC ligands were synthesized based on a method reported by Weiss et al³⁹. Two equivalents of carbon-disulfide to one equivalent of the appropriate para-substituted aniline (Aniline, OMeth-Aniline, and F-Aniline) were added into excess concentrated ammonium hydroxide at 0 °C and stirred overnight. The resulting powder were washed with chloroform and dried under vacuum and characterized by NMR.

Film preparation and ligand exchange

QDs were drop-casted onto borosilicate glass microscope slip covers. Stock solutions of X-PTC in methanol were prepared at 10mM, 15mM, and 20mM. The glass

slip covers coated with QDs were put into the solution overnight for ligand exchange. Uv-Vis spectroscopy was used for exciton dynamic studies.

Preparation of CdSe-sensitized p-GaP electrode

The p-GaP electrode was first etched using concentrated HCl for 30 s and then soaked in HCl-neutralized $(\text{NH}_4)_2\text{S}$ for 6 hrs. Rinsed with water thoroughly and dried with N_2 flow, the electrode was immersed in CdSe quantum dots hexanes solution for 20 min. In order to form a monolayer of quantum dots on GaP surface, the loosely attached quantum dots were removed by thoroughly rinsing with hexanes. Subsequently, the quantum dots sensitized p-GaP electrode was soaked in 10% v/v EDA methanol solution for 10 min for ligand exchange before being used for photoelectrochemical measurements. After obtaining the CdSe-EDA/p-GaP photoresponse spectra, the CdSe sensitized GaP electrodes were further merged in the appropriate PTC Methanol solution [15mM] overnight for ligand exchange. External quantum yield measurements were performed subsequently.

Preparation of p-GaP electrodes and Photoelectrochemical and spectroscopic measurements

Preparation of p-GaP electrodes and the conditions of photoelectrochemical and spectroscopic measurements in this section are same as they are in chapter one.

2.3 Results and discussions

A combination of optical and photoelectrochemical studies has shown that exchanging the native surfactant ligands (TOPO) of CdSe QDs with PTC ligands can shift the excitonic dynamic and further enable the hole injection from CdSe to GaP. Figure 2.2 a shows that after treatments of PTC in methanol solution, CdSe-PTC QDs have demonstrated a red shift up to 20 nm. Equation 1 describes an empirical fitting function of the diameter of CdSe QDs in terms of their excitonic position⁴⁴. Based on calculation, the original size of CdSe-TOPO was 5.29 nm radius. After ligand exchange, the calculated radius was up to 5.60 nm. Figure 2.2 b illustrates a set of photoelectrochemical studies in terms of external quantum yield measurement. All three measurements (Black: bare p-GaP, Red: p-GaP/CdSe/EDA, and Blue: p-GaP/CdSe/PTC) were performed by using the same electrode, same calibration curve, and same conditions. Due to the instrumental filter switch, there was an artificial peak at 570 nm. However, between the red(p-GaP/CdSe-EDA) and black(bare p-GaP) curve, the 560-580 nm range did not show photoresponse, which means that, theoretically, the delocalized holes were not injected from the valence band of CdSe to the valence band of GaP OR the hole injection process was not observed by external quantum yield measurement due to the convolution between the photoreponse profile of CdSe and GaP. Blue curve shows an increased area within 560-580 nm. Hypothetically, these increased signals should be attributed to the additional charge carriers coming from CdSe. Besides, after 610 nm, all three curves coincide with each other and go towards zero, which further indicates that the PTC treatments have shifted the excitonic peaks of CdSe from the original 570 nm to near 600 nm and enabled hole injection processes within this specific range. Additionally,

the increased photoresponse appeared within a range that is matching with the exciton dynamic of the surface modified CdSe depicted in UV-Vis spectrum (Figure 2.1 a). Figure 2.2 c more clearly shows an increased signal at 580 nm and 600 nm between the before-ligand-exchange CdSe sensitization and the after-ligand-exchange CdSe sensitization. In Figure 2.1 a, the wavelength range of excitation states are also consistent with such observations.

Equation 1⁴⁴:

$$D(\text{nm}) = (-6.6521 \times 10^{-8})\lambda^3 + (1.9557 \times 10^{-4})\lambda^2 - (9.2352 \times 10^{-2})\lambda + 13.29$$

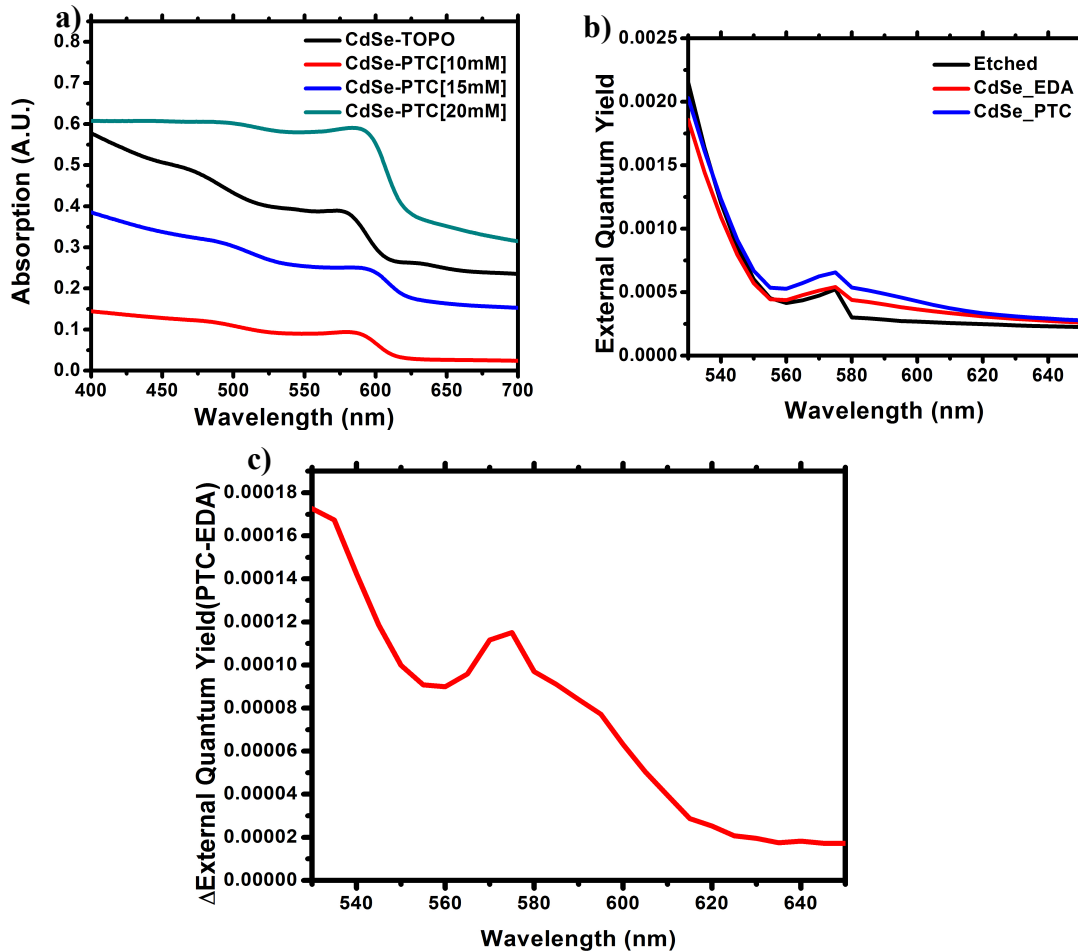


Figure 2.2. a) UV-Vis absorption spectra of CdSe quantum dots with TOPO native ligand (black line) and with PTC ligands in different concentrations. b) External quantum yield spectra for (black) a p-GaP (100) photoelectrode coated with a layer of CdSe with ethyldiamine ligand (black) and phenyldithiocarbamate ligand (red). c) External quantum yield difference between p-GaP/CdSe-EDA and p-GaP/CdSe-PTC.

Figure 2.3 shows a set of Time-resolved photoluminescence decay measurements. Based on equation 2²⁰, when deposited onto insulating glass, CdSe QDs capped with TOPO has shown an average decay time of 2.407 ns. When deposited on GaP, CdSe-TOPO has displayed an average decay time of 2.653 ns. Nearly same photoluminescence decay times demonstrate that the same exciton relaxation pathway may be operative for these two samples. However, after the treatment of ligand exchange, the CdSe-PTC on glass has demonstrated an average decay time of 9.599 ns, while on GaP, an average decay time of 8.110 ns has been observed. Based on calculation, a 1.489 ns difference shows that a new exciton-relaxing pathway may have been generated. Theoretically, if light stimulated hole of CdSe on GaP has been injected into GaP, the photoluminescence decay for CdSe should be faster than the CdSe on Glass samples due to the transfer mechanism of charge carriers. Based on observations, the experimental data is consistent with this hypothesis.

Equation 2²⁰:
$$\frac{\alpha_1\tau_1^2 + \alpha_2\tau_2^2 + \alpha_3\tau_3^2}{\alpha_1\tau_1 + \alpha_2\tau_2 + \alpha_3\tau_3}$$

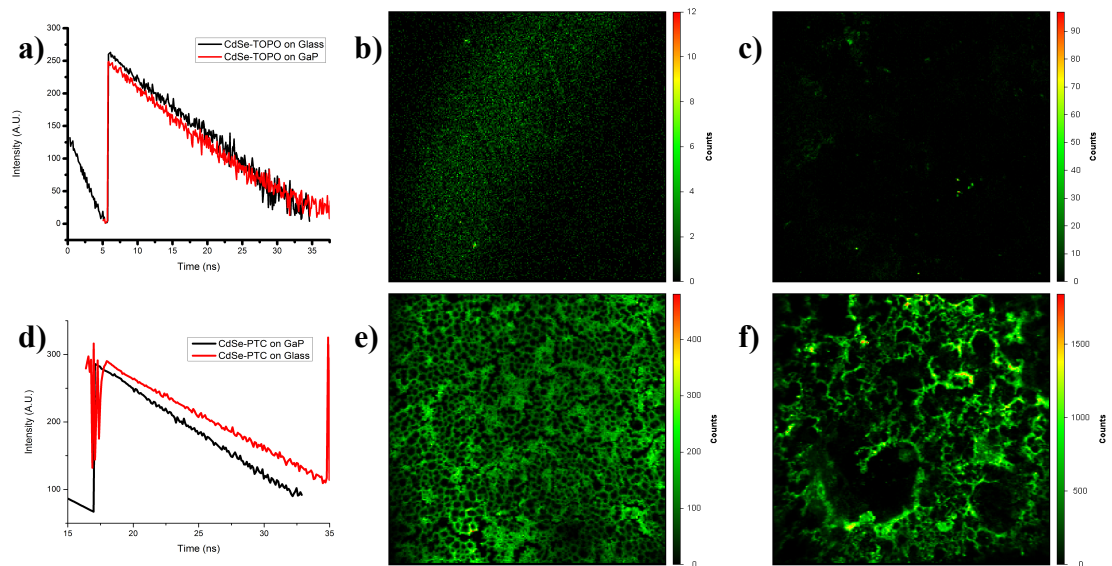


Figure 2.3. a) Time-resolved photoluminescence decays measured from absorbed CdSe quantum dots with TOPO native ligands on (red line) GaP and on (black line) glass. b,c,e,f) Fluorescence image of CdSe on glass, GaP, CdSe-PTC on glass, and GaP. d) Time-resolved photoluminescence decays measured from absorbed CdSe quantum dots with PTC ligands on (red line) glass and on (black line) GaP.

As what discussed in introduction part, the coupling effect between the HOMO of PTC and the valence band edge of QDs can result in the excitonic shift of QDs. If the PTC molecule is para-substituted with an electron-withdrawing group, the inductive effect can lower the HOMO energy level of PTC. Hypothetically, the coupling effect should be stronger so that the bathochromic shift should be more severe. If the PTC molecule is para-substituted with an electron-donating group, the HOMO energy level of PTC should be increased. The coupling effect should lead to a less obvious bathochromic shift. Figure 2.4 a shows a set of UV-Vis absorption spectra of CdSe after treatment of OMeth-PTC ligand exchange. Methoxy group is an electron-donating group. The HOMO energy level of this para-OMeth-PTC ligand should be higher than that of PTC ligand. Theoretically, the weak coupling effect between p-OMeth-PTC and CdSe QDs should not generate severe bathochromic shift in UV-Vis spectra. Figure 2.4 a is consistent with this hypothesis. If the exciton dynamic of QDs is not altered, in photoresponse measurements, both before-ligand-exchange and after-ligand-exchange CdSe/p-GaP pairs should not show hole injections because the originally synthesized QDs are too small and the hole injection is thermodynamically forbidden. Figure 2.4 b is also consistent with this hypothesis. Both of such observations are consistent with literatures³⁹.

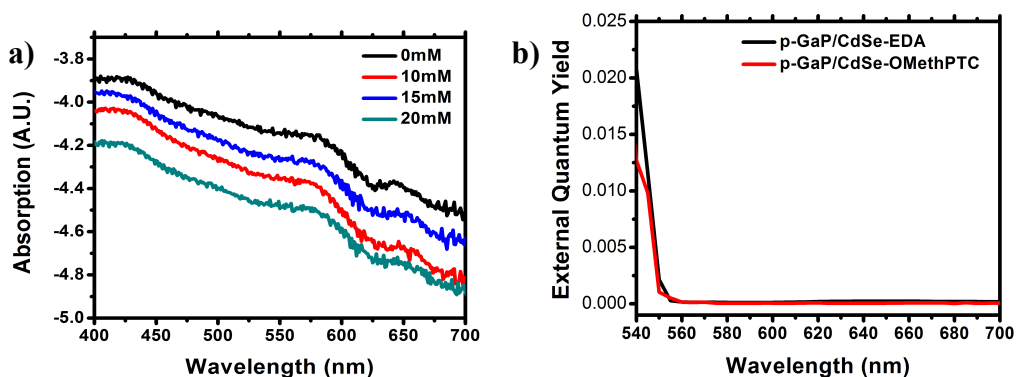


Figure 2.4. a) UV-Vis absorption spectra of CdSe quantum dots with TOPO native ligand (black line) and with PTC ligands in different concentrations. b) External quantum yield spectra for (black) a bare p-GaP (100) photoelectrode (black line) and a p-GaP (100) photoelectrode coated with a layer of CdSe with ethyldiamine ligand (red) and PTC ligand (blue).

Figure 2.5 shows a collection of UV-Vis spectra of CdSe-FPTC. After ligand exchange, a red shift up to 40 nm has been observed, which is higher than the observed shift in CdSe-PTC. Based on Equation 1, the increased radius after ligand exchange is 1.32 nm. The CdSe-PTC samples have 0.31 nm of increased radius. These observations are consistent with the coupling theory previously stated and depicted in literatures^{38, 42}. Figure 2.5 b shows the external quantum yield comparison. Black line is the p-GaP/CdSe sensitization with TOPO surface ligand. There is no observable sensitization signal within 550-600 nm range due to the small sizes of synthesized quantum dots. After surface modification, according to the UV-Vis spectra, quantum dots have shown excitonic peaks shifted to higher wavelength. Accordingly, in quantum yield spectra, additional signals have been observed within this range. Using same electrodes, calibrations, and physical conditions to eliminate instrumental interferences performed both of the measurements.

In this entire study, all observed quantum yield are relatively lower than that in p-GaP CdSe sensitization with EDA ligand in chapter one. This can be attributed to the

nature of long molecular length and bulky molecular structure of phenyldithiocarbamate ligand. Several studies have shown that organic surfactants can separate individual quantum dots and prevent efficient charge transport at the interface^{36, 45-46}. The relatively shorter molecular length of ethylenediamine molecules and better conductivity of amine group may have provided a better charge transfer pathway compared with the phenyldithiocarbamate molecule at the interface between GaP and CdSe.

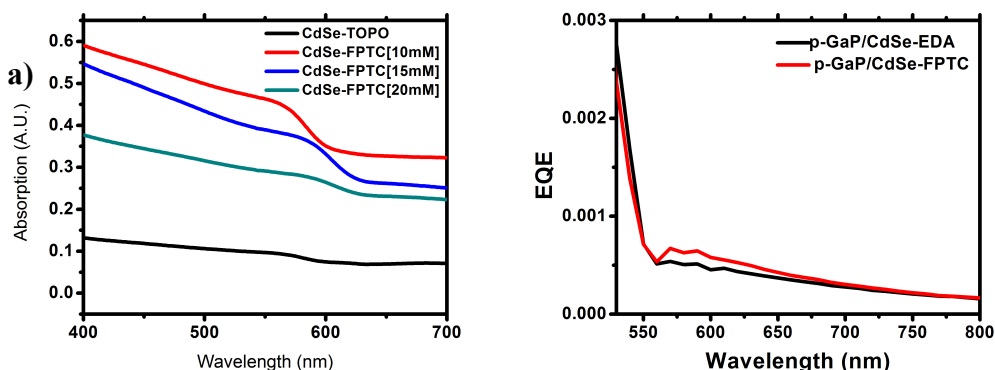


Figure 2.5. a) UV-Vis absorption spectra of CdSe quantum dots with TOPO native ligand (black line) and with F-PTC ligands in different concentrations. b) External quantum yield spectra for (black) a p-GaP (100) CdSe-TOPO photoelectrode and a p-GaP (100) photoelectrode coated with a layer of CdSe with FPTC (red).

2.4 Conclusions

A systematic collection of optical and electrochemical measurements have demonstrated that exchanging the native surface ligand of CdSe QDs with phenyldithiocarbamate will red shift the excitonic peak of QDs. Before ligand exchange, the small CdSe QDs, which have exciton peak at 550 nm did not show increased signals in photoresponse measurement due to the convolution between their exciton dynamic and the GaP's photoresponse signature. After ligand exchange, the increased area within the sub-band range should indicate the occurrence of hole injection from CdSe to GaP. Sensitization range is also consistent with the exciton position of the surface modified QDs.

References

1. Sambur, J. B.; Parkinson, B., CdSe/ZnS core/shell quantum dot sensitization of low index TiO₂ single crystal surfaces. *J. Am. Chem. Soc.* **2010**, *132* (7), 2130-2131.
2. Choi, D.; Rowley, J. G.; Parkinson, B., Dye Sensitization of n and p Type Gallium Phosphide Photoelectrodes. *J. Electrochem. Soc.* **2012**, *159* (11), H846-H852.
3. Leschkes, K. S.; Divakar, R.; Basu, J.; Enache-Pommer, E.; Boercker, J. E.; Carter, C. B.; Kortshagen, U. R.; Norris, D. J.; Aydil, E. S., Photosensitization of ZnO nanowires with CdSe quantum dots for photovoltaic devices. *Nano Lett.* **2007**, *7* (6), 1793-1798.
4. Plass, R.; Pelet, S.; Krueger, J.; Grätzel, M.; Bach, U., Quantum dot sensitization of organic-inorganic hybrid solar cells. *J. Phys. Chem. B* **2002**, *106* (31), 7578-7580.
5. Wang, Z.; Shakya, A.; Gu, J.; Lian, S.; Maldonado, S., Sensitization of p-GaP with CdSe Quantum Dots: Light-Stimulated Hole Injection. *J. Am. Chem. Soc.* **2013**, *135* (25), 9275-9278.
6. Ferrere, S.; Zaban, A.; Gregg, B. A., Dye sensitization of nanocrystalline tin oxide by perylene derivatives. *J. Phys. Chem. B* **1997**, *101* (23), 4490-4493.
7. Chitambar, M.; Wang, Z.; Liu, Y.; Rockett, A.; Maldonado, S., Dye-sensitized photocathodes: efficient light-stimulated hole injection into p-GaP under depletion conditions. *J. Am. Chem. Soc.* **2012**, *134* (25), 10670-10681.
8. Grätzel, M., Dye-sensitized solar cells. *Journal of Photochemistry and Photobiology C: Photochemistry Reviews* **2003**, *4* (2), 145-153.
9. O'regan, B.; Grätzel, M., A low-cost, high-efficiency solar cell based on dye-sensitized. *Nature* **1991**, *353*, 737-740.
10. Law, M.; Greene, L. E.; Johnson, J. C.; Saykally, R.; Yang, P., Nanowire dye-sensitized solar cells. *Nat. Mater.* **2005**, *4* (6), 455-459.
11. Grätzel, M., Solar energy conversion by dye-sensitized photovoltaic cells. *Inorg. Chem.* **2005**, *44* (20), 6841-6851.
12. Mor, G. K.; Shankar, K.; Paulose, M.; Varghese, O. K.; Grimes, C. A., Use of highly-ordered TiO₂ nanotube arrays in dye-sensitized solar cells. *Nano Lett.* **2006**, *6* (2), 215-218.
13. Hod, I.; González-Pedro, V.; Tachan, Z.; Fabregat-Santiago, F.; Mora-Seró, I.; Bisquert, J.; Zaban, A., Dye versus quantum dots in sensitized solar cells: participation of quantum dot absorber in the recombination process. *The Journal of Physical Chemistry Letters* **2011**, *2* (24), 3032-3035.
14. Nozik, A., Quantum dot solar cells. *Physica E: Low-dimensional Systems and Nanostructures* **2002**, *14* (1), 115-120.
15. Sun, W.-T.; Yu, Y.; Pan, H.-Y.; Gao, X.-F.; Chen, Q.; Peng, L.-M., CdS quantum dots sensitized TiO₂ nanotube-array photoelectrodes. *J. Am. Chem. Soc.* **2008**, *130* (4), 1124-1125.
16. Gao, X.-F.; Li, H.-B.; Sun, W.-T.; Chen, Q.; Tang, F.-Q.; Peng, L.-M., CdTe quantum dots-sensitized TiO₂ nanotube array photoelectrodes. *J. Phys. Chem. C* **2009**, *113* (18), 7531-7535.
17. Norris, D.; Bawendi, M., Measurement and assignment of the size-dependent optical spectrum in CdSe quantum dots. *Phys. Rev. B* **1996**, *53* (24), 16338.
18. Norris, D.; Sacra, A.; Murray, C.; Bawendi, M., Measurement of the size dependent hole spectrum in CdSe quantum dots. *Phys. Rev. Lett.* **1994**, *72* (16), 2612.

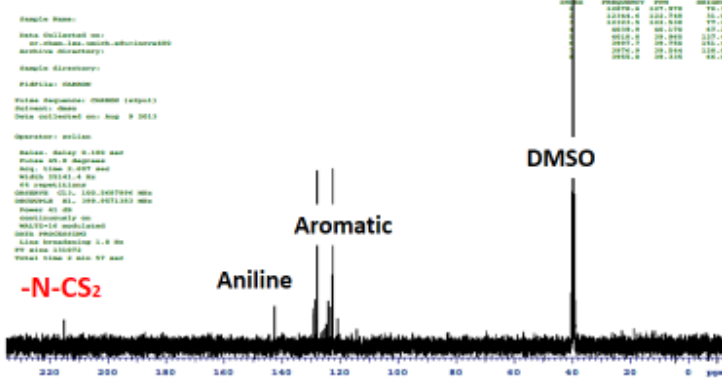
19. Jumabekov, A. N.; Deschler, F.; Böhm, D.; Peter, L. M.; Feldmann, J.; Bein, T., Quantum Dot Sensitized Solar Cells with Water-soluble and Air-stable PbS Quantum Dots. *J. Phys. Chem. C* **2014**.
20. Kongkanand, A.; Tvrđy, K.; Takechi, K.; Kuno, M.; Kamat, P. V., Quantum dot solar cells. Tuning photoresponse through size and shape control of CdSe-TiO₂ architecture. *J. Am. Chem. Soc.* **2008**, *130* (12), 4007-4015.
21. Chang, C.-C.; Chen, J.-K.; Chen, C.-P.; Yang, C.-H.; Chang, J.-Y., Synthesis of Eco-Friendly CuInS₂ Quantum Dot-Sensitized Solar Cells by a Combined Ex Situ/in Situ Growth Approach. *ACS Appl. Mater. Interfaces* **2013**, *5* (21), 11296-11306.
22. Yu, H.; Bao, H.; Zhao, K.; Du, Z.; Zhang, H.; Zhong, X., Topotactically Grown Bismuth Sulfide Network Film on Substrate as Low-Cost Counter Electrodes for Quantum Dot-Sensitized Solar Cells. *J. Phys. Chem. C* **2014**.
23. Robel, I.; Kuno, M.; Kamat, P. V., Size-dependent electron injection from excited CdSe quantum dots into TiO₂ nanoparticles. *J. Am. Chem. Soc.* **2007**, *129* (14), 4136-4137.
24. Amelia, M.; Lincheneau, C.; Silvi, S.; Credi, A., Electrochemical properties of CdSe and CdTe quantum dots. *Chem. Soc. Rev.* **2012**, *41* (17), 5728-5743.
25. Frame, F. A.; Osterloh, F. E., CdSe-MoS₂: A quantum size-confined photocatalyst for hydrogen evolution from water under visible light. *J. Phys. Chem. C* **2010**, *114* (23), 10628-10633.
26. Peng, X. G.; Manna, L.; Yang, W. D.; Wickham, J.; Scher, E.; Kadavanich, A.; Alivisatos, A. P., Shape control of CdSe nanocrystals. *Nature* **2000**, *404* (6773), 59-61.
27. Peng, Z. A.; Peng, X., Mechanisms of the Shape Evolution of CdSe Nanocrystals. *J. Am. Chem. Soc.* **2001**, *123* (7), 1389-1395.
28. Myung, N.; Bae, Y.; Bard, A. J., Effect of surface passivation on the electrogenerated chemiluminescence of CdSe/ZnSe nanocrystals. *Nano Lett.* **2003**, *3* (8), 1053-1055.
29. Green, M., The nature of quantum dot capping ligands. *J. Mater. Chem.* **2010**, *20* (28), 5797-5809.
30. Anderson, N. C.; Hendricks, M. P.; Choi, J. J.; Owen, J. S., Ligand exchange and the stoichiometry of metal chalcogenide nanocrystals: spectroscopic observation of facile metal-carboxylate displacement and binding. *J. Am. Chem. Soc.* **2013**, *135* (49), 18536-48.
31. Anderson, N. C.; Owen, J. S., Soluble, Chloride-Terminated CdSe Nanocrystals: Ligand Exchange Monitored by ¹H and ³¹P NMR Spectroscopy. *Chem. Mater.* **2012**, *25* (1), 69-76.
32. Murray, C. B.; Kagan, C.; Bawendi, M., Synthesis and characterization of monodisperse nanocrystals and close-packed nanocrystal assemblies. *Annu. Rev. Mater. Sci.* **2000**, *30* (1), 545-610.
33. Talapin, D. V.; Lee, J.-S.; Kovalenko, M. V.; Shevchenko, E. V., Prospects of colloidal nanocrystals for electronic and optoelectronic applications. *Chem. Rev.* **2009**, *110* (1), 389-458.
34. Leutwyler, W. K.; Bürgi, S. L.; Burgl, H., Semiconductor clusters, nanocrystals, and quantum dots. *Science* **1996**, *271* (5251), 933-937.
35. Nozik, A. J.; Beard, M. C.; Luther, J. M.; Law, M.; Ellingson, R. J.; Johnson, J. C., Semiconductor quantum dots and quantum dot arrays and applications of multiple

- exciton generation to third-generation photovoltaic solar cells. *Chem. Rev.* **2010**, *110* (11), 6873-6890.
36. Owen, J. S.; Park, J.; Trudeau, P.-E.; Alivisatos, A. P., Reaction Chemistry and Ligand Exchange at Cadmium– Selenide Nanocrystal Surfaces. *J. Am. Chem. Soc.* **2008**, *130* (37), 12279-12281.
37. Aruda, K. O.; Tagliacruzchi, M.; Sweeney, C. M.; Hannah, D. C.; Schatz, G. C.; Weiss, E. A., Identification of parameters through which surface chemistry determines the lifetimes of hot electrons in small Au nanoparticles. *Proceedings of the National Academy of Sciences* **2013**, *110* (11), 4212-4217.
38. Weiss, E. A., Organic Molecules as Tools To Control the Growth, Surface Structure, and Redox Activity of Colloidal Quantum Dots. *Acc. Chem. Res.* **2013**, *46* (11), 2607-2615.
39. Frederick, M. T.; Amin, V. A.; Swenson, N. K.; Ho, A. Y.; Weiss, E. A., Control of exciton confinement in quantum dot-organic complexes through energetic alignment of interfacial orbitals. *Nano Lett* **2013**, *13* (1), 287-92.
40. Knowles, K. E.; Peterson, M. D.; McPhail, M. R.; Weiss, E. A., Exciton Dissociation within Quantum Dot–Organic Complexes: Mechanisms, Use as a Probe of Interfacial Structure, and Applications. *J. Phys. Chem. C* **2013**, *117* (20), 10229-10243.
41. Frederick, M. T.; Amin, V. A.; Cass, L. C.; Weiss, E. A., A Molecule to detect and perturb the confinement of charge carriers in quantum dots. *Nano Lett.* **2011**, *11* (12), 5455-5460.
42. Frederick, M. T.; Amin, V. A.; Weiss, E. A., Optical Properties of Strongly Coupled Quantum Dot–Ligand Systems. *The Journal of Physical Chemistry Letters* **2013**, *4* (4), 634-640.
43. Peterson, M. D.; Cass, L. C.; Harris, R.; Edme, K.; Sung, K.; Weiss, E. A., The Role of Ligands in Determining the Exciton Relaxation Dynamics in Semiconductor Quantum Dots. *Annu. Rev. Phys. Chem.* **2013**, (0).
44. Yu, W. W.; Qu, L.; Guo, W.; Peng, X., Experimental determination of the extinction coefficient of CdTe, CdSe, and CdS nanocrystals. *Chem. Mater.* **2003**, *15* (14), 2854-2860.
45. Zhang, Y.; Schnoes, A. M.; Clapp, A. R., Dithiocarbamates as capping ligands for water-soluble quantum dots. *ACS Appl. Mater. Interfaces* **2010**, *2* (11), 3384-3395.
46. Liu, D.; Wu, W.; Qiu, Y.; Lu, J.; Yang, S., Chemical conjugation of fullerene C60 to CdSe nanocrystals via dithiocarbamate ligands. *J. Phys. Chem. C* **2007**, *111* (48), 17713-17719.

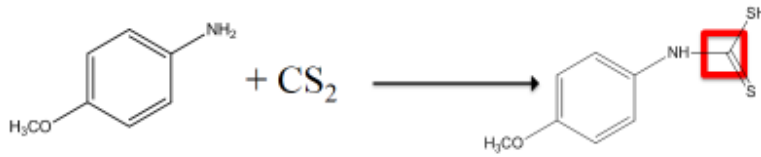
Appendix



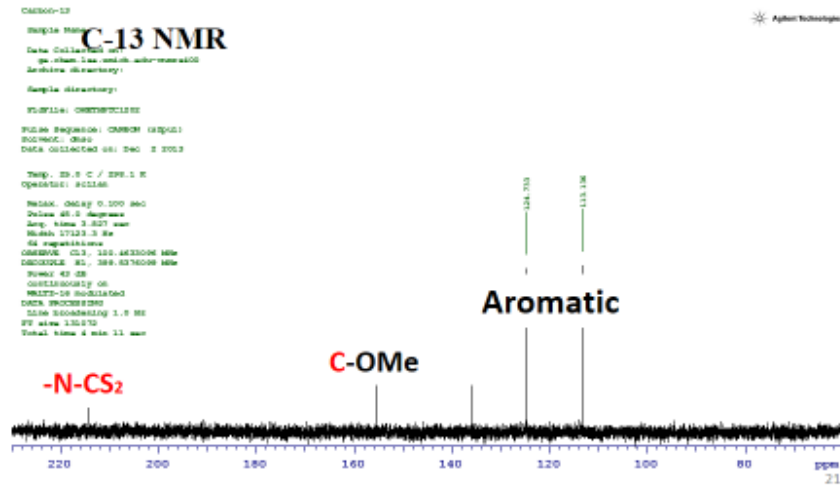
C-13 NMR



9

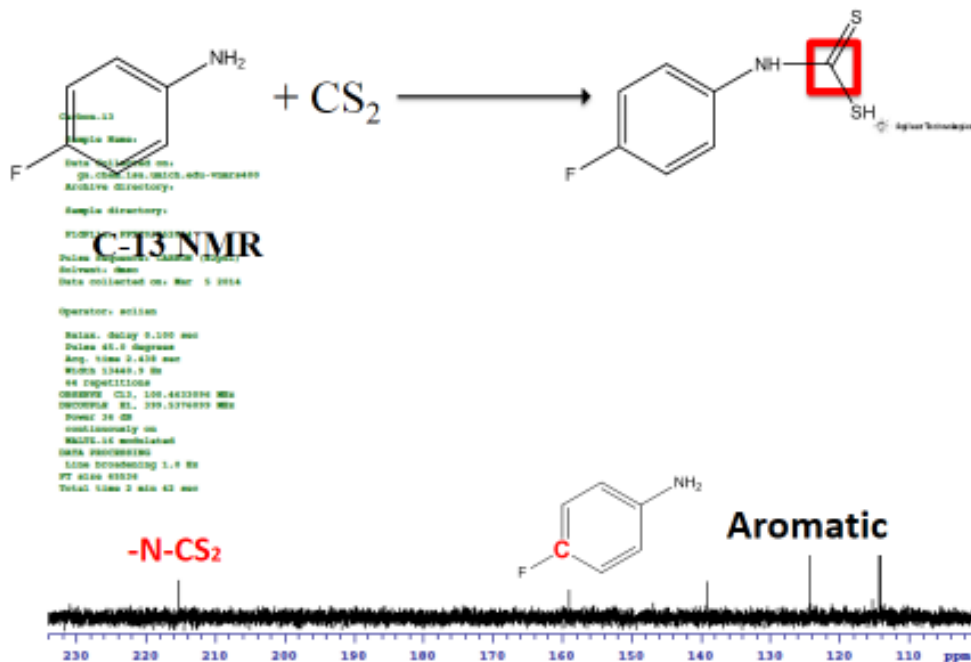


C-13 NMR



Aphor Technologies

21



21

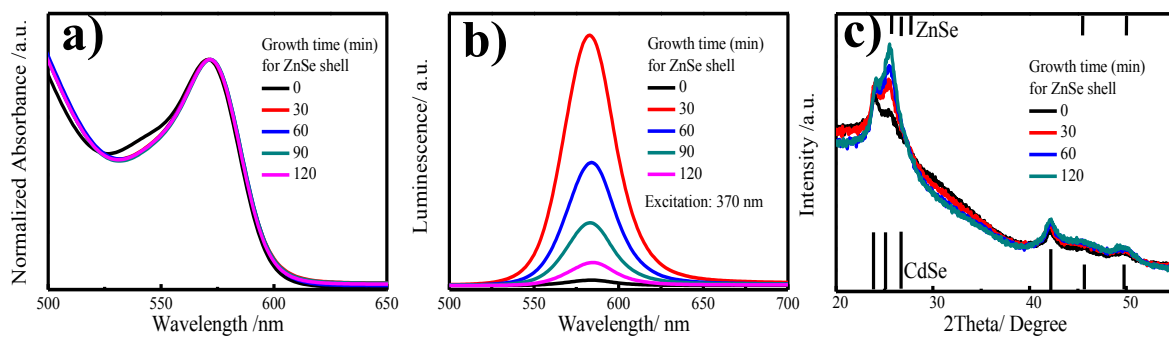


Figure 3.1⁴. (a), (b) and (c) Absorption, luminescence and x ray diffraction spectra of CdSe with different ZnSe shell thickness. Samples for XRD measurement were prepared by drop-casting CdSe hexanes solution on glass substrate.

⁴ Reprinted with permission from (Wang, Z.; Shakya, A.; Gu, J.; Lian, S.; Maldonado, S. *J. Am. Chem. Soc.* **2013**, *135* (25), 9275-9278). Copyright (2014) American Chemical Society